Directed Single Molecule Diffusion Triggered by Surface Energy Gradients

Pierre Burgos,[†,‡,§] Zhenyu Zhang,[†,⊥] Ramin Golestanian,[†,‡] Graham J. Leggett,[‡] and Mark Geoghegan[†,*]

[†]Department of Physics and Astronomy, University of Sheffield, Sheffield S3 7RH, U.K., and [‡]Department of Chemistry, University of Sheffield, Sheffield S3 7HF, U.K. [§]Present address: Central Laser Facility, Rutherford Appleton Laboratory, Chilton, Didcot, Oxfordshire OX11 0QX, UK. [⊥]Present address: Department of Chemistry, University of Sheffield, Sheffield S3 7HF, UK.

ABSTRACT We demonstrate the diffusion of single poly(ethylene glycol) molecules on surfaces which change from hydrophilic to hydrophobic over a few micrometers. These gradients in surface energy are shown to drive the molecular diffusion in the direction of the hydrophilic component. The polymer diffusion coefficients on these surfaces are measured by fluorescence correlation spectroscopy and are shown to be elevated by more than an order of magnitude compared to surfaces without the surface energy gradient. Along the gradient, the diffusion is asymmetric, with diffusion coefficients ~100 times greater in the direction of the gradient than orthogonal to it. This diffusion can be explained by a Stokes—Einstein treatment of the surface-adsorbed polymer.

KEYWORDS: fluorescence correlation spectroscopy · poly(ethylene glycol) · diffusion · single molecule · nanopatterning

The control of single molecules is of considerable interest in areas of molecular assembly such as the control of individual chemical reactions and interactions, single molecular sensing, advanced therapeutics where specific targeting is envisaged, and molecular computers. Although it is possible to mechanically assemble structures,[1] molecular self-propulsion can be obtained by the use of the appropriate gradients. For example, asymmetric catalysis in a solution has been used to drive microspheres through a fluid medium.[2] Surface energy gradients can be used on the macro- and microscale to drive mass transport. For molecular motion, the exploitation of gradients in chemical microreactors may be envisaged; laminar flow in microchannels to control chemical reactions at a specified location has been demonstrated.[3] The use of gradient surfaces in cell biology includes the process by which bacteria exploit a gradient in cellular adhesion receptors to move in the direction of greater nutrient concentration, a process known as haptotaxis.[4] As an example of biomimetic haptotactic motion, adhesion gradients have been exploited to demonstrate motion in vesicles on charged surfaces.[5]

The movement of single molecules on surfaces illustrates the effect of a confining interface. Important early studies were limited to translational diffusion of dye molecules in two dimensions within polymeric films.[6] Although one can extrapolate the diffusion behavior to zero film thickness, such studies can only be considered quasi-two-dimensional at best. Large molecules, such as polymers, are perhaps better suited to experimental study because the time scales of diffusion are more accessible and also because there is more control over other experimental parameters such as their size and chemical composition. Early measurements on DNA diffusion[7] showed a simple behavior, with a diffusion coefficient which scaled with the inverse of the chain size, N. Such a simple result belies the rather complex system of interactions that existed between the DNA and its cationic substrate. An altogether simpler system is that of poly(ethylene glycol) (PEG) on a solid hydrophobized silicon surface. Here the polymer was noted to be adsorbed flat on the surface with a "pancake" structure and a coefficient of diffusion scaling as $N^{-3/2}$.[8,9] The stronger power law behavior of the PEG diffusion with molecular mass indicates that the DNA was much less confined on the surface compared to the PEG.

In this article, we show how a compositional gradient directs the movement of single PEG chains. We have used a simple photolithographic method to create micrometer-sized gradients in monolayer concentration capable of driving significantly anisotropic diffusion so that single molecule motion is directed along a gradient from a hydrophobic to a hydrophilic surface. This diffusion along the gradient is also elevated by

*Address correspondence to mark.geoghegan@sheffield.ac.uk.

Received for review July 8, 2009 and accepted September 3, 2009.

Published online September 23, 2009.
10.1021/nn900991r CCC: $40.75

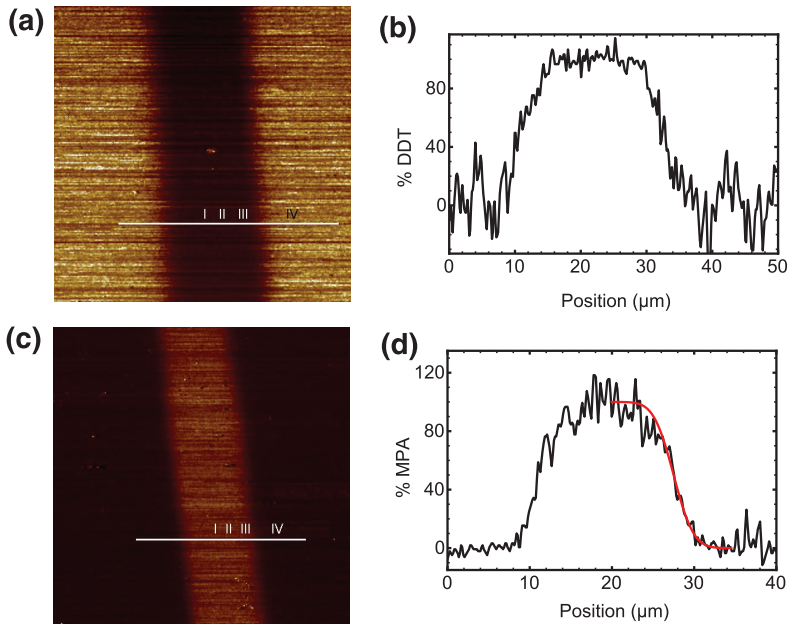

Figure 1. FFM data for (a) a DDT channel and (c) an MPA channel. The concentrations of DDT and MPA are shown in (b) and (d) from line scans for the respective channels. The concentrations were obtained from the line scans as described previously.[39] Each compositional cross section is calculated from a single trace−retrace loop extracted from a single scan line orthogonal to the gradient. The positions I, II, III, and IV mark the approximate points along the channel at which FCS data were obtained. The full curve in (d) is a simulation of the data used to provide the surface energy gradient for an analysis of the results.

between 1 and 2 orders of magnitude compared to that on homogeneous surfaces. We thus demonstrate that single polymer molecules are remarkably responsive to gradients several orders of magnitude larger than the unperturbed size of the polymer. In an aqueous solution, we allowed (PEG) chains to adsorb onto gradient surfaces and measured the surface diffusion of the molecules using fluorescence correlation spectroscopy (FCS). The diffusion of dye-labeled molecules into and out of the (1 fL) confocal volume is detected by the fluorescence of the diffusing molecule.[10] Because FCS is used to detect fluctuations in fluorescence, it works best as a single molecule technique. The shape of the decay of the measured autocorrelation function contains information on the type of motion of the particle, such as whether it is a two- or three-dimensional Brownian diffusion, and how fast the particle is diffusing. It can even measure anisotropy in the diffusion, a possibility exploited in the current work. FCS also allows a measurement of the concentration of labeled particles within the confocal volume because the initial amplitude of the autocorrelation function $G(\tau = 0)$ varies with the inverse of the number of molecules inside the detection volume. We also describe force spectroscopy experiments to realize the conformational behavior of PEG on the pure hydrophobic and hydrophilic surfaces. We used self-assembled monolayers of dodecanethiol (henceforth DDT) and mercaptopropanoic acid (MPA) as model hydrophobic and hydrophilic surfaces, respectively. Dynamic force spectroscopy is used to obtain the energy of adhesion of the PEG to the MPA surface.

RESULTS

Fluorescence Correlation Spectroscopy Diffusion Measurements. The diffusion of monodisperse carboxyrhodamine (Rh6G)-labeled PEG chains of 5 kDa was first studied in solution and calibrated against a Rh6G standard. The diffusion coefficient obtained, 115 ± 5 $\mu m^2/s$, is in agreement with previously published data for chains of similar size.[8]

Labeled polymers were then allowed to adsorb onto the pure and gradient surfaces and their diffusion coefficients measured. For surface diffusion measurement, the possibility of the simultaneous measurement of bulk diffusion cannot be eliminated. This is because the axial length of the confocal volume is ~1.5 μm, and this volume is centered (±100 nm) on the gold surface, so any measurement of surface diffusion must include diffusion in the water above the monolayer. This can be readily accounted for in the FCS analysis where curve fitting of the autocorrelation data reveals components with different correlation times characteristic of free diffusion (<100 μs) as well as motion along the surface (500 to 30 000 μs).

For both pure (hydrophilic and hydrophobic) SAM layers, a range of values was measured for the surface diffusion coefficient, from 0.2 to 0.8 $\mu m^2/s$ for DDT and from 1 to 9 $\mu m^2/s$ for MPA. The diffusion coefficients for Rh6G−PEG on the hydrophobic DDT surface are similar to those of PEG on a hydrophobic surface of octadecyltriethoxysilane.[8,9] In fact, our measurements have been extended to a hydrophobic perfluorodecanethiol monolayer with a diffusion coefficient very close to that of the DDT, 0.45 ± 0.08 $\mu m^2/s$. Similarly, another carboxylic-group-terminated monolayer, mercaptoundecanoic acid, gave a result of 4.2 ± 0.5 $\mu m^2/s$, similar to that on the MPA surface. To test the effect of the presence of both CH_3 and COOH groups at the surface, measurements were also made on a mixed SAM made with the molar ratio of 2 DDT/1 MPA. A diffusion coefficient of 1.0 ± 0.1 $\mu m^2/s$ was measured, intermediate between the values obtained for the pure surfaces. Although phase separation may occur on these mixed SAM surfaces,[11] we do not expect this to occur on a large enough scale to affect this result.

The surface coverage of the polymer on the two surfaces was similar with 5.4 ± 1.0 and 5.0 ± 0.4 molecules/μm^2 on DDT and MPA, respectively. There is no reason to expect the number of adsorbed molecules on the two surfaces to be equal because this will be governed by the different surface energies, the number of adsorbed contact points, and the time that each

molecule spends on the surface, which we refer to below as the *dwell* time. We therefore believe that it is coincidence that these numbers are similar and draw no conclusions from it.

In order to measure surface diffusion on the gradient between the hydrophobic and hydrophilic surfaces, we used nominally identical channels to ensure reproducibility and aid comparison. Figure 1a shows a friction force microscopy (FFM) image of a ~6 μm DDT channel on an MPA surface, with the DDT coverage marked in a line scan in Figure 1b. By a suitable marking of the surface, we were able to locate the channel for the optical FCS experiments and made measurements of surface diffusion at four points: one relatively central (I), where the surface should consist of pure DDT; one on the MPA-functionalized surface outside of the gradient (IV); and two points (II and III) within the gradient channel. Although the broad results that we describe are reproducible, we cannot build up a detailed picture of the diffusion coefficient as a function of position on the channel on account of the lack of resolution that we have in relocating the exact position in the channel, where we estimate an uncertainty of ±0.5 μm. FCS data and fits are shown in Figure 2a for PEG diffusion on and around a gradient. As can be seen from the results shown in Figure 2b, data from the pure SAMs either side of the gradient are the same as those from the homogeneous surfaces; the diffusion coefficient of PEG on (methyl-terminated) DDT in the center of the channel was measured as 0.45 ± 0.05 μm²/s and on MPA (away from the channel) as 4.7 ± 0.4 μm²/s. However, the diffusion coefficients measured at points II and III were markedly different. In particular, significant anisotropy was observed in measurements of the diffusion coefficient, which is attributed to the effect of the gradient. In one experiment, the orthogonal surface diffusion coefficients at position II were 23 and 1.5 μm²/s, whereas at position III, they were 56 and 0.7 μm²/s. The smaller of these two values in both cases is of the same order as the diffusion on the homogeneous surface, but the larger value is very much larger than that measured for either surface in the absence of a gradient. For the two DDT channels that were measured, the ratios of the diffusion coefficients in the two orthogonal directions were, respectively, 33 and 16 for position II and 80 and 50 for position III, a substantial anisotropy. Theory, discussed below, supports the intuitively appealing suggestion that the larger diffusion coefficients correspond to diffusion along the gradient.

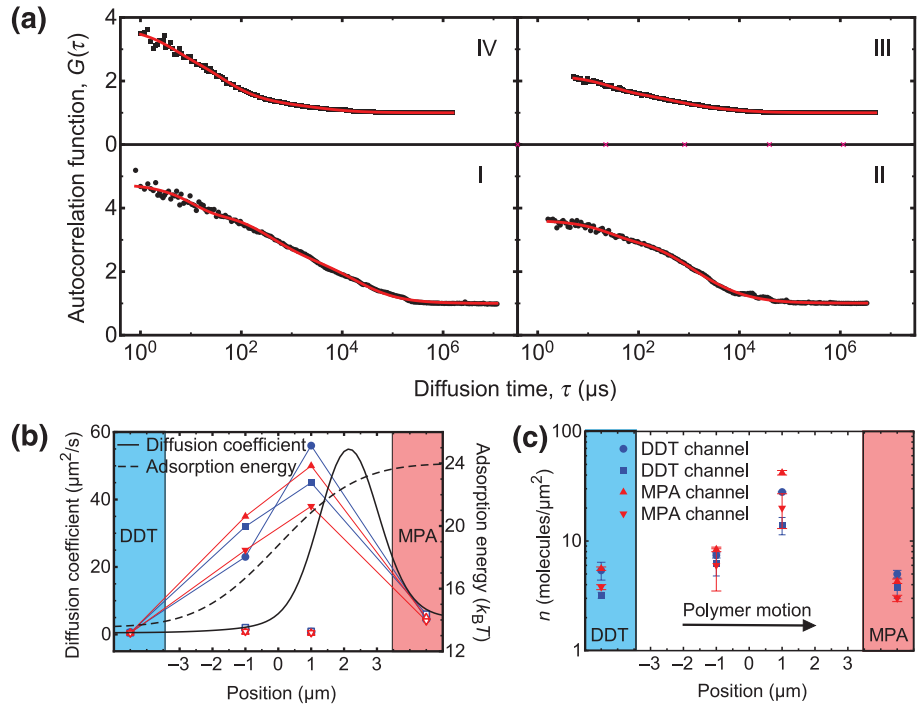

Figure 2. (a) FCS data and fits for rhodamine 6G end-labeled PEG on (I) DDT and (IV) MPA. The channel is DDT within an MPA matrix. The curves II and III are for a gradient between the two surfaces, with II containing more DDT than III. These locations are shown in Figure 1a. The fits (shown in red) are of a very high quality. (b) Diffusion coefficients as a function of position in the gradient are plotted for diffusion along the gradients (filled symbols) and along the channels (open symbols). The uncertainty in the distance between points within the gradient (~6 μm wide) is estimated at about ± 0.5 μm. The diffusion coefficients on the pure surfaces either side of the gradient do not correspond to an actual position. Measurements are presented for four surfaces: two hydrophobic channels and two hydrophilic. The legend for the experimental results is as in (c). Also shown is the adsorption energy as a function of distance along the gradient, assuming polymer adsorption energies of 13.5 k_BT (to DDT) and 24 k_BT (to MPA) and the fit to the FFM data shown in Figure 1d. The solid line is the diffusion coefficient as a function of distance calculated from using these adsorption energies and the theoretical analysis described in the text. (c) Number of Rh6G−PEG molecules/μm² as a function of position within the gradient.

There was also an increase in the number of molecules on the surface at point II and point III. For example, for the DDT channels, at II we measured 7.4 ± 0.4 molecules/μm² on one gradient and 6.3 ± 1.5 molecules/μm² on a similar gradient. At point III, this value increased further to 28.0 ± 0.4 (and 13.9 ± 2.5) molecules/μm². For an MPA channel, the diffusional motion also exhibited pronounced anisotropy, with an increase in the number of adsorbed molecules in the gradient region. The adsorbed amounts for all four channels measured are plotted in Figure 2c. We have observed the same trend on different samples regardless of whether we were measuring diffusion on MPA or DDT channels.

Single Molecule Force Spectroscopy. In order to explain the polymer diffusion on the gradients, it is important to understand how the PEG interacts with the pure

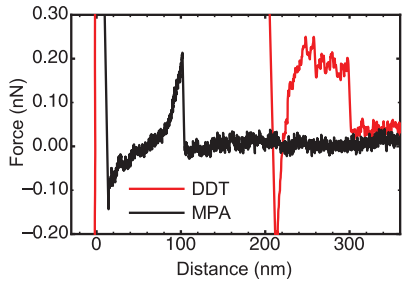

Figure 3. Typical force spectroscopy data showing the interaction between 20 kDa PEG chains attached to the AFM tip and a SAM-covered surface during retraction of the tip. Here, there is only one pulling event on the MPA surface, indicating few monomer−surface contact points. The adhesion to the DDT surface is illustrated by a plateau in the data, indicating that the chain has a pancake conformation on the surface. The DDT data are shifted by ~200 nm due to the cantilever bending because of the hydrophobic interaction between the tip and the surface.

surfaces when adsorbed. An understanding of the conformation of PEG on both DDT and MPA can be obtained using single molecule force spectroscopy. For these experiments, thiol-terminated PEG was adsorbed on a gold-coated atomic force microscope (AFM) tip in solutions dilute enough to provide single molecule studies. The PEG had a molecular mass of 20 kDa, which was the smallest molecular weight for which we were able to obtain useful data. Tips on which PEG had adsorbed were brought into contact with the monolayer-coated surfaces, and the force exerted on the cantilever as it was retracted from the surface was measured as a function of distance from that surface.

Typical force curves from DDT and MPA are shown in Figure 3. The force curves for hydrophobic DDT surfaces exhibit multiple unloading events, indicating that the PEG chain had multiple contact points with the surface. In contrast, few contacts (or typically just one) were observed with MPA. The length of the interaction of PEG with the DDT surface was greater than that with MPA, again suggesting more contact points. The large adhesion force between the tip and the DDT surface is due to a hydrophobic interaction caused by the bending of the cantilever on the surface.[12] We conclude that the PEG chain has a "train-like" conformation on DDT, whereas it prefers extending into liquid from the surface to lying flat on the hydrophilic MPA.

Dynamic Force Spectroscopy. To obtain a true thermodynamic adsorption energy, dynamic force spectroscopy can be performed. Dynamic force spectroscopy is noted for its ability to measure interaction energies between the surface and tip very accurately. An oscillating AFM cantilever presents a harmonic potential away from the surface, but when van der Waals (or other) interactions with the surface become significant, they perturb the harmonic potential, affecting the frequency of the AFM tip, which is now determined by tip−sample distance and resonance amplitude.[13] By varying the perpendicular (*z*-) piezo velocity, one can vary the loading and unloading rate of the polymer on the surface. As for the single molecule force spectroscopy experiments, 20 kDa thiol-terminated PEG was adsorbed from dilute solution onto an AFM tip, which was brought into contact with an MPA surface at different loading rates. The *z*-piezo velocities varied between 80 and 8596 nm/s. The different speeds allow for a variation in the ability of the AFM experiment to overcome the activation energy that inhibits desorption of the sample from the surface, and this variation in turn allows us to isolate the contribution of the activation energy from the thermodynamic surface adsorption energy.[14] Here, the optical lever sensitivity and the cantilever spring constant (107.4 pN/nm) were determined before each force measurement by using the thermal method.[15] The loading rate used in dynamic force spectroscopy is the *z*-piezo velocity multiplied by the effective spring constant, K_{eff}, where $1/K_{eff} = 1/K_s + 1/K_c$, in which K_c is the spring constant of the cantilever and K_s is the slope of the pulling-off peak (this can be seen for PEG on the MPA surface in Figure 3). The bond rupture force (the maximum force at each pulling-off event) and the force-loading rate (slope of the force curves before the bond breaks) were extracted from the retraction force curves. Sample preparation was the same as for the single molecule force spectroscopy experiments, and again, a comparison was made using the PEG-coated tip on an uncoated silicon surface, which is a known pure surface that would allow us to test for multiple polymer interactions from the tip on the surface. The experiments were only performed with an MPA surface. For DDT surfaces, the number of single contacts is too large to analyze; the molecule is *peeled* rather than *pulled* from the surface, and the dynamic force spectroscopy experiment is not appropriate.

Evans and Ritchie[16] proposed a simple model which treats the unbinding event as a kinetic process of the escape from a potential under the influence of external loading force. The dependence of the rupture on the logarithm of the loading rate is fitted by a line to obtain the width (in pm) of the energy barrier causing bond rupture.[17] The relation between rupture force and the loading rate of AFM cantilever is described by

$$F = \frac{k_B T}{\chi_\beta} \ln(r) + \frac{k_B T}{\chi_\beta} \ln\left(\frac{\chi_\beta}{K_d k_B T}\right) \quad (1)$$

in which F is the rupture force, which is the desorption force in our study; k_B is the Boltzmann constant; T is the absolute temperature; χ_β is the width (i.e., with units of length) of the energy barrier; r is the loading rate (units of force per unit time); and K_d is the dissociation (escape) rate. It is this dissociation rate that contains the information that we require, *i.e.*, the thermodynamic energy of adhesion, ΔG between the molecular bonds at the surface, given by the Arrhenius relation

$$K_d = f_m \exp\left(\frac{-\Delta G}{k_B T}\right) \quad (2)$$

where f_m is a prefactor dependent on the particular system.

The analysis that we use follows that previously used in earlier dynamic force spectroscopy experiments.[18] In the form presented, eq 1 allows a linear plot of the rupture force as a function of the logarithm of the loading rate, *i.e.*, $F = (m)\ln(r) + \Delta$. Using eqs 1 and 2, we obtain the simple relation

$$\frac{\Delta G}{k_B T} = \ln(m f_m) + \frac{\Delta}{m} \quad (3)$$

The data (for 20 kDa PEG chains) and fit (to eq 1) are shown in Figure 4, with a force (in pN) given by $F = (53 \pm 17)\ln(r) - (237 \pm 175)$. The scatter in the data is typical for these experiments, but, as we shall see, the analysis of the data is largely unaffected by this scatter. (We must *assume* eq 1 because these experiments are clearly insufficient to *prove* the validity of this equation due to the large scatter in the data.) From the fit, we calculate $\chi_\beta = 78$ pm and $K_d = 1.7\ s^{-1}$. To obtain ΔG using eq 3, a value of f_m is required; f_m is a molecular vibration frequency and can have a wide range of values, dependent on the surface and especially the polymer. It has been suggested that for different systems, f_m can vary from 10^7 to $10^{10}\ s^{-1}$,[19] which limits the accuracy of this method. In fact, because ΔG is proportional to the logarithm of f_m, the effect of this variation in f_m is not so important, and similarly, the large scatter in the data also does not critically affect the value of ΔG. The lower limit is applicable to complex proteins with slow unfolding rates, so we should expect the 20 kDa PEG to have a much larger value of f_m, perhaps between 10^9 and $10^{10}\ s^{-1}$. The form of eq 3 clarifies the robustness of the analysis to both the scatter in the data and the uncertainty in the value of f_m; $\ln(mf)$ dominates the value of ΔG, but Δ/m controls the error to the extent that uncertainty in $\ln(mf)$ may be neglected. Because $\ln(mf)$ is the larger term, the large uncertainty in Δ is less significant than might otherwise be expected, and because we require the logarithm of m, the effect of the error in m is not so significant. We obtain $\Delta G = 16 \pm 4$, 20 ± 4, and $23 \pm 4\ k_B T$ for $f = 10^7$, 10^9, and $10^{10}\ s^{-1}$, respectively.

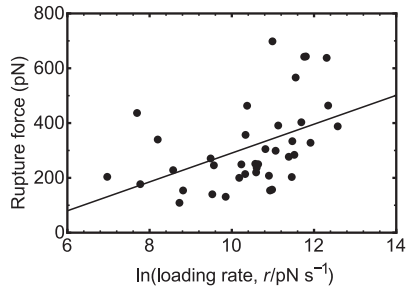

Figure 4. Scatter plot of measured rupture forces at different loading rates. Loading rate was determined from the slope of the force−distance curve immediately preceding the rupture event. The full line shows the fit (in pN) to the experimental data as $F = (53 \pm 17)\ln(r) - (237 \pm 175)$.

The value of ΔG obtained in this way does not refer to individual monomer contacts but rather to a single contact.[20] It is important to note that our dynamic force spectroscopy experiments, like our single molecule force spectroscopy experiments, revealed a limited number of contact points (usually just one) of the PEG with MPA. This does not mean that multiple contacts did not exist, but merely that one ethylene glycol monomer not in contact with the surface cannot be distinguished with the resolution of the experiment. If we consider multiple contact points as identical bonds in parallel, we can then simply assume that the desorption energy is shared equally by all of the bonds responsible for the adsorption. The single contact may nevertheless contain a number of monomers, and if we are to take the literature value of the adsorption energy of ethylene glycol monomers in contact with silica (1.2 $k_B T$)[21] as the same as that for MPA, we assume that a PEG train on the MPA surface consists of ~18 monomers.

DISCUSSION

The reduced diffusion coefficient of the polymers adsorbed on either surface compared to the bulk can be understood using an analogy to the diffusion of proteins in a membrane, described by the Saffman−Delbrück equation,[22] which, with reasonable assumptions, can explain a diffusion coefficient some 2 orders of magnitude smaller on the surface than in bulk solution.

Differences in molecular conformation provide a satisfactory explanation of the different diffusion coefficients on the two surfaces. The "pancake" structure on the DDT allows only two-dimensional motion.[9] This structure has been verified by Monte Carlo simulations[23] as well the force spectroscopy experiments described above. Other systems also show the same effect, with poly(*N*,*N*-dimethyl acrylamide) more likely to adsorb flat on a silicon oxide surface at low pH, representing a more hydrophobic surface, than at high pH, where the oxide layer is negatively charged and thus hydrophilic.[24] However, in this latter example, the adsorption is greater for the more hydrophobic (low pH) oxide surface, indicating the complex three-way interactions that need to be accounted for in the adsorption of polymers from solution. In the case of the adsorption onto MPA, it is perhaps surprising that the PEG does not also form a pancake structure. However, the interaction of water with MPA will compete with the polymer for hydrogen bonds at the surface. Furthermore, the adsorption of PEG onto MPA is expected to take place *via* (strong) hydrogen bonding with undissociated carboxyl groups. Bonding will be impeded by the presence of carboxylate anions on the surface and

by the hydrophobic nature of the methylene units of the PEG. This complex set of interactions can probably only effectively be modeled by simulations, and although demonstrations on carboxylic acid surfaces appear to be lacking, some work has been performed using silica as a model surface.[25] A detailed understanding of the nature of PEG adsorption onto MPA surfaces would be aided by a pH-dependent study.

The larger diffusion coefficient measured on the MPA surface relates to the polymer conformation through the polymer friction coefficient. If we use a simple Stokes−Einstein definition of the diffusion, without any prejudice as to the polymer conformation, we have $D = k_BT/\zeta$, where ζ is a surface energy- and conformation-dependent polymer (surface) friction coefficient. This means that the diffusion coefficients on the different surfaces will be related through the ratio of the two surface friction coefficients. Certainly, simulations have shown that the monomeric friction coefficients have a very strong influence on surface diffusion, with, unsurprisingly, the smaller friction coefficient being responsible for faster surface diffusion.[26] It is also known from Monte Carlo simulations that a strong monomer adsorption does not preclude rapid motion since the monomer does not need to leave the adsorption potential well in order to move laterally.[27]

The strong anisotropic enhancement of the diffusion coefficient of the polymers adsorbed on the gradient is perhaps surprising. One might expect that the surface energy gradient could elongate the chain into a rod, which would cause an anisotropic diffusion. However, the ratio of the two diffusion coefficients in this case would be close to 2,[28] which is too small to account for our observations. Experimental study of diffusion in temperature gradients (the Soret effect) has shown anisotropic diffusion, and many experimental studies exist.[29,30] Here, however, the ratio of thermal to temperature-induced diffusion is generally considerably less than 10.

In order to understand the directed motion, we need to first consider how an adsorbed polymer responds to a gradient. A polymer that is adsorbed on the surface will experience a net drift as a result of the balance between the gradient in interfacial adsorption energy, ∇W and the net friction (drag) force that opposes this motion. This force balance yields an expression for the drift velocity of the adsorbed polymers as

$$v_d = -\frac{\nabla W}{\zeta} \qquad (4)$$

This drift velocity also indicates that the diffusion is in the direction of the MPA.

The polymer cannot move on the surface for too long, as Gibbs equilibrium with the solution makes polymers adsorb and desorb. We can estimate this dwell time as the time it takes for the polymer to escape from the potential well of the adsorbing surface, which can be calculated as[31]

$$\tau_d = \frac{Nb^2}{2D_0}\left(\exp\left(\frac{W}{k_BT}\right) - \frac{W}{k_BT} - 1\right)\left(\frac{k_BT}{W}\right)^2 \qquad (5)$$

where $D_0 = k_BT/\zeta_m$ is the single monomer diffusion coefficient, with ζ_m a single monomer friction coefficient which we can approximate to $\zeta_m = \zeta_b b/R$ where b and R are monomer and polymer sizes, respectively, and ζ_b is the bulk (solution) polymer friction coefficient. The W-dependent factor $(\exp(W/k_BT) - (W/k_BT) - 1)(k_BT/W)^2$ in eq 5 is a measure of the energy required to escape the potential well caused by adsorption on the surface. The total polymer adsorption energy, W, is the product of the number of monomer contacts and the monomer adsorption energy. Accurate values in the literature are missing for PEG on our particular surfaces, but we can make a reasonable estimate for the adsorption on DDT from literature values. Given the consistency between our diffusion coefficients on DDT and those measured for PEG of a similar molecular mass on an octadecyltriethoxysilane (OTS) surface,[9] it seems reasonable to assume the OTS adsorption energy of 0.17 k_BT per monomer, corresponding to a total adsorption energy for the polymer on OTS of 5.7 k_BT for $N = 48$ is applicable to our system;[9] we therefore obtain a polymer adsorption energy of ~13.5 k_BT for $N = 114$ (*i.e.*, 5 kDa). For adsorption onto MPA, the dynamic force spectroscopy data suggest that a polymer adsorption energy between 20 ± 4, and 23 ± 4 k_BT is appropriate. Although these dynamic force spectroscopy experiments were performed with 20 kDa PEG, there was typically only one anchoring event in these experiments, and it seems reasonable to assume that 5 kDa PEG would also have only one anchoring point on MPA. We assume here that the conformation of the polymer at the contact with the surface is independent of chain length and so the dynamic force spectroscopy result for 20 kDa PEG is therefore directly transferable to the 5 kDa PEG. The nearest literature values for comparison are for silica, with an adsorption energy of ~1.2 k_BT per monomer and, with approximately 25% of monomers in contact with the surface,[21] a polymer adsorption energy of ~30 k_BT.

Before calculating surface diffusion coefficients, we shall need to consider the diffusion coefficient in bulk solution, which is given by $D_b = k_BT/\zeta_b = k_BT/(6\pi\eta R)$, where $\eta = 0.8$ mPa · s is the viscosity of water, and $R = bN^{1/2}$. Using $N = 114$, $b = 0.7$ nm,[32] we calculate $D_b = 90$ μm²/s, which supports our experimental value of 115 ± 5 μm²/s, although we note that $R = bN^{1/2}$ represents the size of the chain in a theta (neutral) solvent. The distance traveled on the surface in one dwell period is given by $\delta = v_d\tau_d$, so we can estimate a correction to the longitudinal diffusion coefficient of $\Delta D_x = v_d^2\tau_d$. We estimate the surface friction coefficient by tak-

ing ratios of the diffusion coefficient in bulk solution, D_b, to that on the appropriate surface (MPA or DDT), and taking the literature polymer adsorption energies (i.e., 13.5 and 30 k_BT for OTS (here DDT) and silica (as a proxy for MPA), respectively), which follow the position-dependent measured gradients, and assuming that the surface friction coefficient changes proportionally with the adsorption energy, we obtain an extremely large maximum excess diffusion coefficient $\Delta D_x \approx 1.7 \times 10^4$ $\mu m^2/s$, which is achieved closer to the MPA surface than to the DDT one; the exponential in the dwell time ensures that the excess diffusion coefficient is not symmetric around the midpoint of the gradient. Nevertheless, these results are very sensitive to the polymer adsorption energy; in Figure 2b, we plot the diffusion coefficient using a smaller polymer-MPA adsorption energy of 24 k_BT, which is consistent with the dynamic force spectroscopy data, and with which we obtain a maximum diffusion coefficient similar to that measured by FCS.

It should be noted that this is not a quantitative proof of the mechanism of motion; we do not have the experimental resolution to measure the diffusion coefficient carefully as a function of distance along the gradient, especially given the exponential dependence of τ_d on the adsorption energy and the uncertainties in the friction coefficient. Nevertheless, we are encouraged that reasonable values of adsorption energy provide diffusion coefficients consistent with our experimental data and so qualitatively explain our findings.

The question of why the polymer concentration increases on the gradient does not easily follow from the increased diffusion coefficients. As stated above, it is probably coincidental that the pure MPA and DDT surfaces have similar adsorbed amounts; there are far fewer monomer−surface contacts on the MPA surface than on the DDT surface, and each molecule is believed to remain much longer on the MPA surface than on the DDT one. Since the surface concentrations of PEG on MPA and DDT either side of the gradient must be at an equilibrium value, any PEG traveling on the gradient must be compensated by the diffusion current, caused by an excess of polymer at the DDT side of the gradient. This is easily understood if we take the net polymer flux to be zero:

$$J = -D\nabla n + nv_c = 0 \qquad (6)$$

where n is the number density of polymers and v_c is the convective flow speed. Integrating this equation (assuming constant D) yields a number density profile that is controlled by the Boltzmann weight of the surface adsorption energies along the gradient.

CONCLUSION

We have shown that micrometer-sized surface gradients direct the diffusion of single polymer molecules. We have measured increases in diffusion by up to a factor of 80 compared to diffusion in the orthogonal lateral direction, which can be explained by assuming the adsorbed polymer moves following Stoke's law on the surface, the diffusion coefficient of which is controlled by a larger dwell time at its end closer to the hydrophilic side of the gradient. These surface gradients also increase the adsorption of the polymers to the surface.

MATERIALS AND METHODS

Force Spectroscopy. Gold-coated AFM cantilevers (MLCT, Veeco probe, CA) were incubated in dilute solution of 10^{-8} mol/L methoxy PEG (20 ± 2 kDa, Jenkem Tech. China) to attach a limited number of thiol-terminated PEG chains to the tip. This solution is dilute enough so that a satisfactory number of single molecule experiments were performed; in more concentrated solutions, multiple pulling events would be recorded. These polymers have a larger molecular mass than those used for the fluorescence correlation spectroscopy (FCS) studies because the 5 kDa PEG used in the FCS experiments is too small, and 20 kDa is the smallest molecular mass for which we could obtain reliable results. A molecular force probe (MFP-1D, Asylum Research, Santa Barbara, CA) was used to produce curves of force against PEG-coated tip−sample surface (DDT or MPA) distance. A full description of this procedure is given elsewhere.[33] In order to ensure that we were performing single molecule experiments, a comparison was made using the PEG-coated tip on an uncoated silicon surface, which is a known pure surface that would allow us to test for multiple polymer interactions from the tip on the surface.

Creation of Micrometer-Sized Gradient Channels. The creation of synthetic gradients on different length scales has been reviewed elsewhere.[34,35] Here, a facile method was used to create surface compositional gradients on very small length scales with no surface topographic effects. Alkanethiol molecules adsorb spontaneously onto gold surfaces through the thiol headgroup forming a SAM with a packing area of 0.21 nm^2 per molecule.[36] Exposure of a carboxylic acid-terminated SAM (or a methyl-terminated SAM) to UV light (244 nm) in the presence of oxygen leads to selective photo-oxidation, and the mechanism and kinetics of modification have been extensively characterized using surface spectroscopic and other methods.[37] Oxidation products are weakly bound at the surface and readily displaced.[37] If exposure is carried out using a UV laser coupled to an optical fiber, a gradient of exposure results at the perimeter of the exposed region. Immersion in a solution of a methyl-terminated thiol (or a carboxylic acid-terminated thiol) leads to displacement of the oxidation products and a mixed, gradient region with a composition that reflects the gradient of photochemical oxidation free from chemical and topographical artifacts.[37] The oxidized molecules can be replaced with a contrasting alkanethiol in a second solution-phase step.[37] In this way it is possible to create molecular patterns using scanning near-field optical lithography.[38] In a recent work[39] we showed that it is possible to fabricate a hydrophilic (hydrophobic) channel by sweeping the etched optical fiber up and down a hydrophobic (hydrophilic) SAM at a speed of 10 $\mu m\ s^{-1}$ and that, at the periphery of the pattern, we can obtain gradients of controlled size by this method. These compositional gradients can be readily characterized by friction force microscopy (FFM).[40] The parameters controlling the size of the gradient include the distance of the fiber from the surface, the intensity of the UV light, and the irradiation time. Here we have created micrometer-sized channels of dodecanethiol (DDT) in a mercaptopropanoic acid (MPA) matrix. The width of the channel is 16 μm and its length 200 μm. The gradient (~6 μm of width either side of the channel) was analyzed using friction force microscopy.[11] Channels with surface energy gradients (from hydrophobic to hydrophilic and *vice versa*)

were prepared. Hydrophilic surfaces were made using pure $HS(CH_2)_2COOH$ (mercaptopropanoic acid, MPA) and the hydrophobic SAM from pure $HS(CH_2)_{11}CH_3$ (dodecanethiol, DDT).

Fluorescence Correlation Spectroscopy. The PEG (of molecular mass 5 kDa, corresponding to a degree of polymerization $N = 114$) with a mono end-labeled fluorescent probe (Rhodamine 6G) was synthesized by Carbomer (San Diego, CA, USA) with a polydispersity of 1.01. A small amount of polymer was diluted in water (chromatographic pure water, Aldrich) to prepare a 10 μM solution. Excess rhodamine dye present in the initial solution (detected by FCS) was removed by overnight ultrafiltration (using a membrane with a 2 kDa threshold). Finally a 10 nM polymer solution was prepared and stored in a fridge. Diffusion of the end-labeled polymer was performed using a Zeiss Confocor 2 fluorescence correlation spectroscopy apparatus combined with an LSM 510 fluorescence confocal microscope. Rhodamine G-labeled poly(ethylene glycol) was excited using the 514 nm line of an argon laser. Fluorescence emission was collected through a 560−615 nm band-pass filter and recorded with an avalanche photodiode. Photobleaching was inhibited by attenuation of the laser using a neutral density filter. Control measurements monitored with 10 μM Rhodamine 6G (Sigma) solutions ensured correct alignment of the confocal optics. Fluorescein isothiocyanate-labeled PEG (again 5 kDa) also gave results in agreement with our Rh6G−PEG values, but was prone to high triplet formation and photobleaching and so was not used in the present study.

For surface measurements, an accurate positioning of the confocal volume on the SAM surface is crucial to record artifact-free correlation curves. Initially, *z*-scanning is performed in steps of 100 nm from the bulk solution toward the gold surface and the desired position on the surface was selected where the signal to noise ratio is maximized using the automated stage positioning of the ConfoCor 2 system. This is particularly important because the use of a gold surface (on which the SAM sits) amplifies the noise, as well as the signal, because it acts as a mirror. A Zeiss incubator was used to control the sample environment at 28 °C. The sample was measured in a specially designed cell and allowed to equilibrate for 40 min before measuring.

The autocorrelation function $G(\tau)$, obtained by the FCS measurements, was used to obtain both the surface density of adsorbed molecules and the diffusion coefficient. The average number of particles inside the confocal volume is related to their brightness and can lead to biased results if this parameter is not taken into account. It is well-known that a metallic surface significantly influences the absorption and emission properties of a fluorophore placed in its vicinity. Nevertheless, with the Rh6G−PEG, neither quenching nor enhancement of the fluorescence was observed, and we have verified that the fluorescence quantum yield on the surface is the same as that in dilute solution. Diffusion on metallic surfaces has been studied recently and is characterized by a supplementary diffusion time in the autocorrelation curve;[41] such a phenomenon is not observed here. Therefore for a single component, the autocorrelation function describing a combination of anisotropic bulk diffusion mixed with a two-dimensional anisotropic surface diffusion is given by

$$G(\tau) = 1 + \frac{G_{triplet}(\tau)}{n}\left(\frac{(1-f)}{\left(1+\frac{\tau}{\tau_{3D}}\right)\sqrt{\left(1+\frac{\tau}{\tau_{3D}S^2}\right)}} + \frac{f}{\sqrt{\left(1+\frac{\tau}{\tau_{D_x}}\right)\left(1+\frac{\tau}{\tau_{D_y}}\right)}}\right) \quad (7)$$

where $G_{triplet}(\tau)$ is the autocorrelation function of the triplet fluorescence decay (which is significant at short times only, $\tau < 15$ μs); f is the fraction of molecules in the confocal volume that are on the surface of the film, the remainder being in the bulk with diffusion time τ_{3D}; S is a calibration parameter ($4 < S < 11$) dependent on the width of the confocal volume (200−250 nm), which is fixed from control measurements using the 10 μM Rh6G solutions; n is the number of dye molecules inside the confocal volume; and τ_{D_x} and τ_{D_y} are the orthogonal surface diffusion times. Clearly, this equation returns to the standard bulk autocorrelation function when the confocal volume is completely immersed in the solution and $f = 0$. It was often the case that surface diffusion completely dominated over bulk diffusion and $f = 1$. For a homogeneous surface, this equation can be simplified with $\tau_{D_x} = \tau_{D_y}$. Data were collected for 10 autocorrelation functions during 50 s and the autocorrelation functions averaged. The correlation functions computed from experimental measurements were fitted to the appropriate models for times superior to 2 μs to avoid complications due to detector afterpulse distortions, which were negligible at these times. Correlation functions with a triplet fraction higher than 15% were discarded as were data where the error on the diffusion coefficient was greater than 10%. Data were analyzed by Levenberg−Marquardt nonlinear least-squares fitting to eq 7, simplified as described above where necessary. Only if fitting could not be achieved with a suitable symmetric surface diffusion, were the orthogonal diffusion coefficients introduced.

Location of the Channel for FCS Measurements. Before photo-oxidation of the monolayer, two crosses were drawn on it using sharp tweezers. The optical fiber delivering 244 nm light for photo-oxidation was scanned back and forth in the area between the crosses forming a channel, with immersion in a second thiol solution providing the necessary surface energy contrast. The two crosses are easily found with the microscope enabling a facile determination of the position of the channel for FCS measurements, limiting our positional sensitivity to within 0.5 μm.

Acknowledgment. We thank the EPSRC (GR/T07473/01) for support. Helpful discussions and correspondence with Peter Olmsted (R.G. and M.G.), Richard Jones (R.G.), and Sebastian Schmidt (Z.Z.) are acknowledged.

REFERENCES AND NOTES

1. Kufer, S. K.; Puchner, E. M.; Gumpp, H.; Liedl, T.; Gaub, H. E. Single-Molecule Cut-and-Paste Surface Assembly. *Science* **2008**, *319*, 594–596.
2. Howse, J. R.; Jones, R. A. L.; Ryan, A. J.; Gough, T.; Vafabakhsh, R.; Golestanian, R. Self-Motile Colloidal Particles: From Directed Propulsion to Random Walk. *Phys. Rev. Lett.* **2007**, *99*, 048102.
3. Kenis, P. J. A.; Ismagilov, R. F.; Whitesides, G. M. Microfabrication inside Capillaries Using Multiphase Laminar Flow Patterning. *Science* **1999**, *285*, 83–85.
4. Carter, S. B. Haptotaxis and the Mechanism of Cell Motility. *Nature* **1967**, *213*, 255–261.
5. Solon, J.; Streicher, P.; Richter, R. P.; Brochard-Wyart, F.; Bassereau, P. Vesicles Surfing on a Lipid Bilayer: Self-Induced Haptotactic Motion. *Proc. Natl. Acad. Sci. U.S.A.* **2008**, *103*, 12382–12387.
6. Hall, D. B.; Torkelson, J. M. Small Molecule Probe Diffusion in Thin and Ultrathin Supported Polymer Films. *Macromolecules* **1998**, *31*, 8817–8825.
7. Maier, B.; Rädler, J. Conformation and Self-Diffusion of Single DNA Molecules Confined to Two Dimensions. *Phys. Rev. Lett.* **1999**, *82*, 1911–1914.
8. Sukhishvili, S. A.; Chen, Y.; Müller, J. D.; Gratton, E.; Schweizer, K. S.; Granick, S. Diffusion of a Polymer 'Pancake'. *Nature* **2000**, *406*, 146.
9. Sukhishvili, S. A.; Chen, Y.; Müller, J. D.; Gratton, E.; Schweizer, K. S.; Granick, S. Surface Diffusion of Poly(ethylene glycol). *Macromolecules* **2002**, *35*, 1776–1784.
10. Eigen, M.; Rigler, R. Sorting Single Molecules: Application to Diagnostics and Evolutionary Biotechnology. *Proc. Natl. Acad. Sci. U.S.A.* **1994**, *91*, 5740–5747.
11. Leggett, G. J.; Brewer, N. J.; Chong, K. S. L. Friction Force Microscopy: Towards Quantitative Analysis of Molecular Organisation with Nanometre Spatial Resolution. *Phys. Chem. Chem. Phys.* **2005**, *7*, 1107–1120.
12. Teschke, O.; de Souza, E. F. Measurements of Long-Range Attractive Forces between Hydrophobic Surfaces and Atomic Force Microscopy Tips. *Chem. Phys. Lett.* **2003**, *375*, 540–546.

13. Hölscher, H.; Allers, W.; Schwarz, U. D.; Schwarz, A.; Wiesendanger, R. Determination of Tip−Sample Interaction Potentials by Dynamic Force Spectroscopy. *Phys. Rev. Lett.* **1999**, *83*, 4780–4783.
14. Butt, H.-J.; Cappella, B.; Kappl, M. Force Measurements with the Atomic Force Microscope: Technique, Interpretation and Applications. *Surf. Sci. Rep.* **2005**, *59*, 1–152.
15. Hutter, J. L.; Bechhoefer, J. Calibration of Atomic-Force Microscope Tips. *Rev. Sci. Instrum.* **1993**, *64*, 1868–1873.
16. Evans, E.; Ritchie, K. Dynamic Strength of Molecular Adhesion Bonds. *Biophys. J.* **1997**, *72*, 1541–1555.
17. Strunz, T.; Oroszlan, K.; Schumakovitch, I.; Güntherodt, H.-J.; Hegner, M. Model Energy Landscapes and the Force-Induced Dissociation of Ligand-Receptor Bonds. *Biophys. J.* **2000**, *79*, 1206–1212.
18. Ray, C.; Brown, J. K.; Akhremitchev, B. B. Single Molecule Force Spectroscopy Measurements of "Hydrophobic Bond" between Tethered Hexadecane Molecules. *J. Phys. Chem. B* **2006**, *110*, 17578–17583.
19. Yang, W. Y.; Gruebele, M. Folding at the Speed Limit. *Nature* **2003**, *423*, 193–197.
20. Evans, E. Probing the Relation between Force-Lifetime- and Chemistry in Single Molecular Bonds. *Annu. Rev. Biophys. Biomol.* **2001**, *30*, 105–128.
21. Trens, P.; Denoyel, R. Conformation of Poly(ethylene glycol) Polymers at the Silica/Water Interface: A Microcalorimetric Study. *Langmuir* **1993**, *9*, 519–522.
22. Saffman, P. G.; Delbrück, M. Brownian Motion in Biological Membranes. *Proc. Natl. Acad. Sci. U.S.A.* **1975**, *72*, 3111–3113.
23. Lai, P.-Y. Statics and Dynamics of a Polymer Chain Adsorbed on a Surface: Monte Carlo Simulation Using the Bond Fluctuation Model. *Phys. Rev. E* **1994**, *49*, 5420–5430.
24. Zhang, Z.; Tomlinson, M. R.; Golestanian, R.; Geoghegan, M. The Interfacial Behaviour of Single Poly(*N*,*N*-dimethylacrylamide) Chains as a Function of pH. *Nanotechnology* **2008**, *19*, 035505.
25. Postmus, B. R.; Leermakers, F. A. M.; Cohen Stuart, M. A. Self-Consistent Field Modeling of Poly(ethylene oxide) Adsorption onto Silica: The Multiple Roles of Electrolytes. *Langmuir* **2008**, *24*, 1930–1942.
26. Ponomarev, A. L.; Sewell, T. D.; Durning, C. J. Surface Diffusion and Relaxation of Partially Adsorbed Polymers. *J. Polym. Sci., Part B: Polym. Phys.* **2000**, *38*, 1146–1154.
27. Milchev, A.; Binder, K. Static and Dynamic Properties of Adsorbed Chains at Surfaces: Monte Carlo Simulation of a Bead-Spring Model. *Macromolecules* **1996**, *29*, 343–354.
28. Levine, A. J.; Liverpool, T. B.; MacKintosh, F. C. Dynamics of Rigid and Flexible Extended Bodies in Viscous Films and Membranes. *Phys. Rev. Lett.* **2004**, *93*, 038102.
29. Platten, J. K. The Soret Effect: A Review of Recent Experimental Results. *J. Appl. Mech.* **2006**, *73*, 5–15.
30. Wiegand, S. Thermal Diffusion in Liquid Mixtures and Polymer Solutions. *J. Phys.: Condens. Matter* **2004**, *16*, R357–R379.
31. Serr, A.; Netz, R. R. Enhancing Polymer Adsorption by Lateral Pulling. *Europhys. Lett.* **2007**, *78*, 68006.
32. Oesterhelt, F.; Rief, M.; Gaub, H. E. Single Molecule Force Spectroscopy by AFM Indicates Helical Structure of Poly(ethylene-glycol) in Water. *New J. Phys.* **1999**, *1*, 6.
33. Seog, J.; Dean, D.; Plaas, A. H. K.; Wong-Palms, S.; Grodzinsky, A. J.; Ortiz, C. Direct Measurement of Glycosaminoglycan Intermolecular Interactions *via* High-Resolution Force Spectroscopy. *Macromolecules* **2002**, *35*, 5601–5615.
34. Genzer, J.; Bhat, R. R. Surface-Bound Soft Matter Gradients. *Langmuir* **2008**, *24*, 2294–2317.
35. Kim, M. S.; Khang, G.; Lee, H. B. Gradient Polymer Surfaces for Biomedical Applications. *Prog. Polym. Sci.* **2008**, *33*, 138–164.
36. Dhirani, A.; Hines, M. A.; Fisher, A. J.; Ismail, O.; Guyot-Sionnest, P. Structure of Self-Assembled Dodecane Thiol on Ag(111): A Molecular Resolution Scanning Tunneling Microscopy Study. *Langmuir* **1995**, *11*, 2609–2614.
37. Leggett, G. J. Scanning Near-Field Photolithography-Surface Photochemistry with Nanoscale Spatial Resolution. *Chem. Soc. Rev.* **2006**, *35*, 1150–1161.
38. Sun, S.; Chong, K. S. L.; Leggett, G. J. Nanoscale Molecular Patterns Fabricated by Using Scanning Near-Field Optical Lithography. *J. Am. Chem. Soc.* **2002**, *124*, 2414–2415.
39. Burgos, P.; Geoghegan, M.; Leggett, G. J. Generation of Molecular-Sized Compositional Gradients in Self-Assembled Monolayers. *Nano Lett.* **2007**, *7*, 3747–3752.
40. Chong, K. S. L.; Sun, S.; Leggett, G. J. Measurement of the Kinetics of Photo-Oxidation of Self-Assembled Monolayers Using Friction Force Microscopy. *Langmuir* **2005**, *21*, 3903–3909.
41. Etienne, E.; Lenne, P.-F.; Sturgis, J. N.; Rigneault, H. Confined Diffusion in Tubular Structures Analyzed by Fluorescence Correlation Spectroscopy on a Mirror. *Appl. Opt.* **2006**, *45*, 4497–4507.